Maladaptative autophagy impairs adipose function in Congenital Generalized Lipodystrophy due to cavin-1 deficiency

Laurence Salle-Teyssières, Martine Auclair, Faraj Terro, Mona Nemani, Solaf M Elsayed, Ezzat Elsobky, Mark Lathrop, Marc Délépine, Olivier Lascols, Jacqueline Capeau, et al.

Maladaptative autophagy impairs adipose function in Congenital Generalized Lipodystrophy due to cavin-1 deficiency

Laurence Salle-Teyssières, M.D., Martine Auclair, Faraj Terro, Ph.D., Mona Nemani, Ph.D., Solaf M Elsayed, M.D., Ezzat Elsobky, M.D., Mark Lathrop, Ph.D., Marc Délépine, Olivier Lascols, Ph.D., Jacqueline Capeau, M.D., Ph.D., Jocelyne Magré, Ph.D, Corinne Vigouroux, M.D., Ph.D.

From Sorbonne Universités, UPMC Univ Paris 6, and Inserm UMR_S938, Centre de Recherche Saint-Antoine, F-75012, Paris, France (L.S-T., M.A., M.N., O.L., J.C., C.V.), Institute of Cardiometabolism and Nutrition (ICAN), Groupe Hospitalier La Pitié-Salpêtrière, F-75013 Paris, France (L.S-T., M.A., O.L., J.C., C.V.), Service d'Histologie et de Biologie Cellulaire, Faculté de Médecine-Université de Limoges (F.T.), AP-HP, Hôpital Tenon, Service de Biochimie et Hormonologie, F-75020, Paris, France (J.C.), Medical Genetics Center, Cairo, Egypt (S.M.E., E.E.), McGill University and Génome Québec Innovation Centre, Montréal, Canada (M.L.), Commissariat à l'Energie Atomique/ Institut de Génomique/ Centre National de Génotypage (CEA/IG/CNG), Evry, France (M.D.), AP-HP, Hôpital Saint-Antoine, Laboratoire Commun de Biologie et Génétique Moléculaires, F-75012, Paris, France (O.L., C.V.), Inserm UMR_S1087, L'Institut du Thorax, F-44007 Nantes, France (J.M.).

Abbreviated title: *PTRF* mutations and maladaptative autophagy

Key terms: PTRF, cavin-1, lipodystrophy, insulin resistance, autophagy, adipocyte differentiation

Word count: Main text, 3798 words; Figures, 5; Table, 1; References, 43

Corresponding author: Corinne Vigouroux, Centre de Recherche Saint-Antoine, Faculté de médecine Pierre et Marie Curie, 27, rue Chaligny, 75012 Paris, France

Funding sources: This work was supported by grants from the French 'Institut National de la Santé et de la Recherche Médicale' (Inserm), 'Aide aux Jeunes Diabétiques' and 'Société Francophone du Diabète'. Laurence Salle-Teyssières was the recipient of a master grant from the Limousin Regional

Health Agency and Mona Nemani received grants from ‘Région Ile-de-France’ and ‘Aide aux Jeunes Diabétiques’.

Disclosure statement: The authors have nothing to disclose.

Precis:

Two new homozygous *PTRF* mutations associated with Congenital Generalized Lipodystrophy induce cellular maladaptative autophagy resulting in insulin resistance and altered adipocyte differentiation.

Abstract

Context: Mutations in *PTRF* encoding cavin-1 are responsible for congenital generalized lipodystrophy type 4 (CGL4) characterized by lipoatrophy, insulin resistance, dyslipidemia and muscular dystrophy. Cavin-1 cooperates with caveolins to form the plasma membrane caveolae, involved in cellular trafficking and signalling and in lipid turnover.

*Objective :*We sought to identify *PTRF* mutations in patients with CGL and to determine their impact on insulin sensitivity, adipose differentiation and cellular autophagy.

Design and patients : We performed phenotyping studies and molecular screening of *PTRF* in two unrelated families with CGL. Cellular studies were conducted in cultured skin fibroblasts from the two probands and from control subjects, and in murine 3T3-F442A preadipocytes. Knockdown of cavin-1 or ATG5 was obtained by siRNA-mediated silencing.

Results: We identified two new *PTRF* homozygous mutations (p.Asp59Val or p.Gln157Hisfs*52) in four patients with CGL4 presenting with generalized lipoatrophy and associated metabolic abnormalities. In probands' fibroblasts, cavin-1 expression was undetectable and caveolin-1 and -2 barely expressed. Ultrastructural analysis revealed a loss of membrane caveolae and the presence of numerous cytoplasmic autophagosomes. Patients’cells also showed increased autophagic flux and blunted insulin signaling. These results were reproduced by *PTRF* knockdown in control fibroblasts and in 3T3-F442A preadipocytes. Cavin-1 deficiency also impaired 3T3-F442A adipocyte differentiation. Suppression of autophagy by siRNA-mediated silencing of *ATG5* improved insulin sensitivity and adipocyte differentiation.

Conclusions: This study showed that cavin-1 deficiency resulted in maladaptative autophagy which contributed to insulin resistance and altered adipocyte differentiation. These new pathophysiological mechanisms could open new therapeutic perspectives for adipose tissue diseases including CGL4.

INTRODUCTION

Congenital generalized lipodystrophies (CGL) represent a group of rare monogenic disorders characterized by an overall defect in adipose tissue development associated with severe insulin resistance, diabetes, dyslipidemia and liver steatosis. CGL is a heterogeneous genetic disease, but the great majority of cases are due to biallelic mutations in either *BSCL2* encoding seipin, a protein involved in adipogenesis and lipid droplet formation, or *AGPAT2* encoding the enzyme 1-acyl-glycerol-3-phosphate acyltransferase-ß involved in the biosynthesis of triglycerides and glycerophospholipids (1). A few cases of CGL have been shown to result from mutations in *CAV1*, encoding caveolin-1 (2,3) or from mutations in *PTRF*, encoding polymerase I and transcript release factor, also known as cavin-1. PTRF mutations are responsible for the association of generalized lipoatrophy and muscular dystrophy, categorized as congenital generalized lipodystrophy type 4 (CGL4) (4-10).

Both cavin-1 and caveolin-1 are required for the formation of caveolae, which are specialized omega-shaped microdomains of the plasma membrane involved in endocytosis, signal transduction, and lipid transport and metabolism (11,12). Cavin-1 is a scaffold protein present in numerous cell types, including myocytes, endothelial cells, fibroblasts and adipocytes, where caveolae are particularly abundant. Cavin-1 has a critical importance for caveolae assembly (11), recruiting caveolins into caveolae and preventing their degradation by the endolysosomal system (13). In addition, cavin-1 colocalizes with caveolin-1 and -2, hormone-sensitive lipase and perilipin-1 at the adipocyte lipid droplet surface, and contributes to the regulation of lipid droplet expandability (12,14-18). Cavin-1 is also present in the cell nucleus, where it participates in transcription processes and regulation of cellular senescence (19).

Few studies have investigated the cellular consequences of CGL4-linked cavin-1 mutations. They were shown to result in a secondary deficiency of caveolins, which could play an important pathophysiological role (2-4,7,8). Accordingly, cavin-1 knock-out in mice recapitulates the phenotype observed in caveolin-1 deficient mice, including lack of cellular caveolae, lipodystrophy and insulin resistance (20-22).

Macroautophagy – hereafter referred to as "autophagy" – is the main cellular pathway for lysosomal degradation of altered proteins and organelles. Autophagy plays a crucial role in protein quality control in a basal state, and contributes to cellular defense when activated in response to stress conditions (adaptative autophagy) (23). Importantly, autophagy has also been shown to regulate lipid metabolism, adipocyte differentiation and insulin sensitivity (24,25). Aberrant regulation of adipose tissue autophagy has been reported in obesity and diabetes (26). Interestingly, caveolin-1 suppression in mice has been shown to overactivate autophagy in stromal cells (22) and adipocytes (27). Caveolin-1 was also demonstrated to regulate autophagy in lung and vascular endothelial cells (28,29). However, the role of cavin-1 in the regulation of autophagy and associated metabolic functions remains to be investigated.

In this study, we identified new *PTRF* mutations in two families with CGL and show that subsequent loss of cavin-1 expression led to autophagy upregulation, resulting in insulin resistance and altered adipocyte differentiation. These novel pathophysiological mechanisms could offer innovative therapeutic perspectives for this severe orphan disease and other adipose tissue diseases associated with maladaptative autophagy.

SUBJECTS AND METHODS

Subjects

Two unrelated patients issued from consanguineous families originating from Egypt and from Switzerland, were referred to Saint-Antoine hospital (Paris, France) for CGL. Clinical, biological, molecular, and cellular studies of the probands and their relatives were performed after full informed consent according to legal procedures.

Phenotype and genotype characterization

Subjects underwent clinical evaluation and routine biological measurements, performed after an overnight 12-h fast. Serum adiponectin and leptin levels were determined by ELISA (Quantikine, R&D Systems, Oxford, UK). Genomic DNA was extracted from peripheral-blood leukocytes. The

entire coding region and splice junctions of genes involved in lipodystrophies (*i.e. BSCL2, AGPAT2, CAV1, PTRF, LMNA, PPARG, AKT2, CIDEC, PLIN1*) were amplified by PCR with specific primers in the two probands (primers sequences are available upon request). Purification of PCR products was performed on Sephadex columns and sequencing used Big Dye Terminator chemistry (Applied Biosystems). *PTRF* was also sequenced in the probands' family members and in 100 unrelated control subjects.

Cellular studies

Primary fibroblast cultures were established from skin biopsies in the two probands and compared to those from two healthy women aged 20 and 33 (30). Murine 3T3-F442A preadipocytes were cultured and induced for adipocyte differentiation during 7 days as described (31).

For **mRNA silencing**, cells were incubated for 6h with 100 pmoles of control (scrambled) siRNA (sc-37007), or a pool of 3-5 specific siRNA targeting murine or human *PTRF* (sc-76294 and sc-76293) or *ATG5* (sc-41446 and sc-41445) (all from Santa Cruz Biotechnology, Santa Cruz, CA, USA), in the provided transfection reagent. Fibroblasts were studied 4 days after mRNA silencing. 3T3-F442A preadipocytes were evaluated 3 days after mRNA silencing (D0, undifferentiated state), then 7 days after adipocyte differentiation (D7).

Western blot analyses were performed on whole cell extracts using specific antibodies listed in **Supplemental Table 1**. Protein detection and semi-quantitative analysis of western blots *versus* beta-actin were performed using ChemiGenius2 Bio-imaging system (Syngene, Cambridge, UK).

Autophagy is characterized by the formation of double-membrane organelles known as autophagosomes, which surround targeted cytoplasmic materials. The trafficking of autophagosomes and then their fusion with lysosomes leads to the degradation of the sequestrated material (32). During this process, the cytosolic protein LC3-I is modified to a lipidated form, LC3-II, which associates to autophagosome membranes and is then submitted to the autophagic flux. We monitored autophagy as previously described, in the presence or not of the autophagic flux blocker bafilomycin A1 (B1793, Sigma-Aldrich) (100 nM for 4h), which inhibits the late phase of autophagy by preventing the fusion between autophagosomes and lysosomes (33). We measured the amount of p62/sequestosome-1, an

autophagy substrate degraded in lysosomes. We also evaluated the rate of conversion of LC3-I to LC3-II (LC3-II-to-LC3-I ratio), which correlates with autophagosome formation, and the levels of LC3-II, which is also degraded in lysosomes.

To study **insulin signaling**, cells maintained for 24h in a serum-free medium were incubated or not with 50 nmol/L human insulin (#I9278, Sigma-Aldrich) for 8min. We evaluated the total protein expression of insulin receptor and of the signalling intermediates extracellular signal-regulated kinase (ERK) 1/2 and Akt as well as their phosphorylated activated forms (**Supplemental Table 1**).

Adipocyte conversion of 3T3-F442A cells was assessed by the expression of adipocyte-specific proteins and by Oil red O-staining of intracellular neutral lipid stores, which was quantified at 520 nm after solubilization in 10% SDS and normalization to the amount of total proteins.

For **mRNA expression studies,** total RNA was isolated from cultured fibroblasts using RNeasy kit (Qiagen, Courtaboeuf, France). cDNA was synthesized using random hexamers and AMV-RT (Promega, Madison, WI, USA) for 60min at 42°C. Real-time PCR was performed with specific primers (available upon request) using the FastStart SYBR Green I mix and the LightCycler detection system (Roche Diagnostics, Meylan, France). TATA box binding protein (TBP) was used for normalization. The relative expression of genes was calculated by the LightCycler Relquant program using comparative C_t method.

Immunofluorescence studies were performed on fibroblasts grown on glass coverslips, after fixation in methanol at -20°C. DAPI (4',6'-di-amidine-2-phenylindole dihydrochloride) was used for nuclear staining. Cells were visualized and images were acquired using Leica SP2 confocal microscope and software.

Ultrastructural analysis by electronic microscopy was performed on cultured fibroblasts fixed in 2.5% glutaraldehyde at 4°C. Cells were rinsed in PBS, post-fixed in 1% osmium tetroxide, dehydrated using graded alcohol series then embedded in epoxy resin. Semi-fine sections (0.5 µm) were stained with toluidine blue. Ultrathin sections (60 nm) were contrasted with uranyl acetate and lead citrate and examined using a JEOL 1010 electron microscope (JEOL, Tokyo, Japan) with an OSIS mega View III camera.

Quantitative results, presented as mean ± SD, were statistically analyzed by non-parametric Mann-

Whitney test using PRISM software (GraphPad Software, Inc, CA, USA). *P* values <0.05 were considered as significant.

RESULTS

Phenotype studies

Proband-1 was a 32-year-old woman, born from consanguineous parents (first-cousins) of Sicilian origin. She presented with paucity of fat and muscular hypertrophy since birth and was diagnosed with generalized lipodystrophy and diabetes at age 12. Despite high doses of insulin (up to 2U/kg/day) associated with pioglitazone (30 mg/day), chronic hyperglycemia persisted (HbA1c: 8.8%) and was complicated by proliferative retinopathy. Acute pancreatitis linked to major hypertriglyceridemia occurred at age 16. The patient had also mild mental retardation diagnosed during early childhood and hypergonadotrophic hypogonadism, with primary amenorrhea and limited breast development (Tanner stage 3). Her height was 158 cm, her weight 48 kg (BMI: 19.2 kg/m^2). Muscular strength was normal but she complained of cramps. *Acanthosis nigricans* was present on neck and axillar folds. Abdominal ultrasonography showed hepatomegaly, and liver steatosis was diagnosed at age 23 on histology. Cardiac examination (including echography and electrocardiogram) was normal. Biological measurements revealed high creatine kinase levels, high triglycerides and low HDL-cholesterol levels, low leptin and adiponectin levels and mild renal insufficiency. Her 60 year-old mother (BMI 21.9, normal physical examination) had type 2 diabetes since age 46. Her 62 year-old father and 35 year-old sister were described as asymptomatic, without lipodystrophy, muscular signs, diabetes, or dyslipidemia. They refused medical examination and molecular analyses.

Proband-2 was a 13-year-old girl at examination. She was born from Egyptian consanguineous parents (first-cousins), with a low birth weight (2000g) at term after an uneventful pregnancy. She was diagnosed with generalized lipodystrophy at age 1, and mild mental retardation at age 10. Her height was 151 cm, her weight 40 kg (BMI: 17.5 kg/m^2, Z-score: -0.47). Spontaneous menarche occurred at age 15 after a normal pubertal development. In addition to typical generalized lipoatrophy, she showed

generalized muscular hypertrophy, pseudoacromegaloid features (enlarged hands and feet, prominent eyebrows' arches), axillar and cervical *acanthosis nigricans*, and liver hypertrophy. Cardiac examination was normal. Biological investigations revealed normal fasting glucose with high insulin levels, slightly elevated liver enzymes, very low levels of leptin and adiponectin, and very high serum creatine kinase, although she did not complain of any muscular symptoms. One of her four sisters died at 2.5 months from respiratory distress. Her two youngest sisters, 2 and 6 years-old, were described with congenital generalized lipoatrophy and muscle weakness, associated with achalasia in the older one. Her 36 year-old mother, 41 year-old father, and 11 year-old sister were asymptomatic and their physical examination was normal.

The main clinical and biological characteristics of the probands and affected relatives are summarized in **Table 1**.

Molecular studies

PTRF sequencing in proband-1 revealed a homozygous c.176A>T transversion in exon 1, predicting a p.Asp59Val substitution in the highly conserved N-terminal leucine-rich domain of cavin-1 (**Fig. 1**). Her mother was heterozygous for the mutation. A homozygous transversion of the last nucleotide of exon 1 (*PTRF* c.471G>C), predicting a Gln-to-His substitution at codon 157, was detected in proband-2 and her two lipodystrophic sisters. Direct sequencing of cDNA derived from proband-2' cultured skin fibroblasts showed that this mutation results in a splicing defect. The frameshift insertion of 143 nucleotides from intron 1, followed by a premature codon stop in exon 2, predicted the synthesis of a mutated truncated protein (*PTRF* p.Gln157Hisfs*52) **(Fig. 1)**. Proband-2' asymptomatic parents and sister were heterozygous for the mutation. The family trees, sequence analyses and alignments are shown in **Fig. 1**. The two *PTRF* mutations were absent in 100 unrelated control subjects (50 of Caucasian and 50 of Egyptian origin) and in the 1000 Genome Project Database. The *PTRF* p.Asp59Val mutation was reported in the Exome Aggregation Consortium (ExAC) Database with an allelic frequency of 0.00001658, in the heterozygous but not the homozygous state (2 alleles among 120646). This mutation was not submitted to ClinVar. It was predicted to be damaging by Polyphen-2,

SIFT and MutationTaster. The truncating mutation *PTRF* p.Gln157Hisfs*52 was not reported in ExAC. No pathological alteration was found in other lipodystrophy-related genes in the two probands (*i.e. BSCL2, AGPAT2, CAV1, PTRF, LMNA, PPARG, AKT2, CIDEC, PLIN1*).

Cell studies

***PTRF*-mutated fibroblasts from the two probands showed decreased number of caveolae and increased autophagic flux**

Cavin-1 protein was not detectable in fibroblasts from the two probands, as shown by western blotting and immunofluorescence microscopy (**Fig. 2A,B**). Cavin-1 mRNA expression was strikingly decreased in fibroblasts from proband-2 but was not modified in proband-1 as compared to control cells (data not shown), suggesting post-translational modifications leading to protein degradation in this case. Protein levels of caveolin-1 and caveolin-2 were decreased (**Fig. 2A**). Electronic microscopy showed, respectively, a decreased number and an absence of plasma membrane caveolae in fibroblasts from proband-1 and -2 as compared to control cells (**Fig. 2C**). In addition, an increased number of autophagic vacuoles was observed in fibroblasts from the probands. Some of these vacuoles, which displayed multimembranous structures, were identified as autophagosomes (**Fig. 2D**).

To further characterize intracellular autophagy in *PTRF*-mutated *vs* control fibroblasts, we evaluated the conversion from soluble microtubules-associated light chain 3 protein (LC3-I) to vacuolar membrane-associated LC3-II, which correlates with autophagosome formation (34). Immunofluorescence detection of LC3 showed an increase in the number of LC3-positive bright puncta, depicting LC3-II associated with autophagosomes, in cells from probands as compared to controls (**Fig. 2B).** Western blot revealed increased LC3-II levels and LC3-II-to-LC3-I ratios, showing that the number of autophagosomes was increased, in patients' versus controls' fibroblasts (**Fig. 2E**). The selective autophagy substrate p62, which is degraded by lysosomes when autophagy is activated, was decreased in patients' versus control cells, in favor of an enhanced autophagic flux (**Fig. 2E**). As expected, blockade of the autophagic flux by bafilomycin A1, which prevents the fusion between autophagosomes, endosomes and lysosomes (33), increased LC3-II-to-LC-I ratio and inhibited

substrate degradation as reflected by increased p62 levels, in both control and mutated fibroblasts (**Fig. 2F**).

Taken together, these results show that patients' fibroblasts with cavin-1 deficiency displayed decreased caveolae formation and increased autophagic flux.

PTRF-mutated fibroblasts from the two probands displayed cellular insulin resistance, and siRNA-mediated _PTRF_ knockdown in control fibroblasts recapitulated increased autophagy and insulin resistance

We evaluated insulin-stimulated activation of the insulin receptor and the insulin signaling intermediates protein kinase B (PKB/Akt) and extracellular-regulated kinases (ERK1/2) in fibroblasts from the two patients and from control subjects. Insulin-induced activation of the signaling proteins was blunted in probands' fibroblasts as compared to controls (**Fig. 3A**).

To determine the involvement of cavin-1 deficiency in increased autophagy flux and insulin resistance, we performed siRNA-mediated silencing of *PTRF* in control fibroblasts. Efficient *PTRF* knockdown also led to a drastic reduction in caveolin-1 and -2 proteins (**Fig. 3B**), and activated the autophagic flux, as shown by an increase in LC3-II level and LC3-II-to-LC3-I ratio and a decrease in p62 level (**Fig. 3C**). In addition, *PTRF* knockdown reduced insulin-activated phosphorylation of Akt and ERK1/2 (**Fig. 3D**).

These results demonstrated that cavin-1 deficiency activated autophagy and reduced insulin response in human fibroblasts.

PTRF silencing in 3T3-F442A preadipocytes activated autophagy, induced insulin resistance and impaired adipocyte differentiation

We then studied the effects of *PTRF* mRNA silencing in murine 3T3-F442A preadipocytes. Cells were evaluated 3 days after siRNA transfection, in the undifferentiated state (D0), and 7 days after induction of differentiation (D7). As observed in fibroblasts, *PTRF* silencing was associated with a decrease in caveolin-1 and caveolin-2 proteins, both at D0 (data not shown) and D7 of differentiation (**Fig. 4A**). *PTRF* knockdown also activated autophagy, as shown by increased LC3-II-to-LC3-I ratio

and decreased p62 protein amount **(Fig. 4A)**. In addition, insulin signaling, studied at D7 of differentiation, was blunted in cavin-1 deficient 3T3-F442A cells. *PTRF* silencing decreased insulin-induced phosphorylation of insulin receptor β-subunit, Akt and ERK1/2, indicating cellular insulin resistance (**Fig. 4B**). Beside, *PTRF* knockdown significantly decreased the total amount of insulin receptor ß-subunit, which also represents a marker of mature adipocytes (1.27 ± 0.14 *vs* 0.66 ± 0.05 arbitrary units (mean ± SD) in control and cavin-1 deficient 3T3-F442A cells, respectively, p=0.05). In accordance, adipocyte differentiation of 3T3-F442A cells, assessed by increased protein expression of key adipocyte transcription factors (C/EBP-α, PPARγ, SREBP-1c) and of the mature adipocyte marker fatty acid synthase (FAS) from D0 to D7, was impaired by *PTRF* knockdown (**Fig. 4C**). Finally, *PTRF* mRNA silencing decreased the ability of differentiating 3T3-F442A cells to store lipids, as indicated by decreased Oil red O-staining at D7 of differentiation (**Fig. 4D**).

Therefore, in 3T3-F442A cells, cavin-1 knockdown was responsible for activation of autophagy, insulin resistance and impaired adipocyte differentiation.

In *PTRF*-mutated fibroblasts from the two probands, suppression of autophagy by *ATG5* knockdown partially reversed cellular insulin resistance

To further investigate the role of increased autophagy in *PTRF* knockdown-induced insulin resistance, we blocked the mRNA expression of ATG5, a key component of the molecular core machinery of autophagy (33), in fibroblasts from probands and controls. As expected, efficient *ATG5* silencing reversed the overactivation of autophagic processes associated with cavin-1 deficiency, as shown by a decreased LC3-II-to-LC3-I ratio and an increased p62 amount in knocked-down versus untreated probands'cells (**Supplemental Fig. 1A**). We also observed that reducing autophagy in patients' fibroblasts significantly increased the amount of p.Asp59Val mutated cavin-1 from proband 1, though it still remained lower than in control cells (**Supplemental Fig. 1A**). This suggests that overactivation of autophagy partially contributed to the posttranslational degradation of this cavin-1 mutant. *ATG5* silencing also increased insulin-induced phosphorylation of Akt and ERK1/2 in patients' fibroblasts (**Fig. 5A**). Importantly, *ATG5* knockdown in control fibroblasts did not significantly alter the LC3-II-

to-LC3-I ratio and p62 level (**Supplemental Fig. 1A**) and the insulin-mediated activation of Akt and ERK1/2 (**Fig. 5A**).

In 3T3-F442A cells, suppression of autophagy by *ATG5* siRNA-mediated silencing reversed *PTRF* knockdown-induced insulin resistance and altered adipocyte differentiation

We then studied the effects of *ATG5* mRNA silencing in murine 3T3-F442A preadipocytes subjected or not to *PTRF* knockdown prior to induction of differentiation. As expected, *PTRF* knockdown-induced activation of autophagy was partially reversed by concomitant *ATG5* silencing, the increased LC3-II-to-LC3-I ratio and decreased p62 levels being partly rescued at D7 of differentiation (**Supplemental Fig. 1B** and data not shown). As observed in patients' fibroblasts, *ATG5* knockdown in 3T3-F442A cells partly reversed the insulin resistance resulting from cavin-1 deficiency, as assessed by increased insulin-mediated phosphorylation of Akt and ERK1/2. Morever, *ATG5* mRNA silencing increased both total protein level and insulin-mediated tyrosine phosphorylation of the insulin receptor ß-subunit in *PTRF* knockdown cells (**Supplemental Fig. 1C**).

In addition, suppression of autophagy by *ATG5* silencing prevented the decrease in C/EBPα, PPARγ, SREBP-1c and FAS proteins induced by cavin-1 deficiency in differentiating 3T3-F442A cells (**Fig. 5B**). In accordance, it also improved the lipid storage capacity of cavin-1 deficient 3T3-F442A cells, evaluated by Oil red O-staining at D7 of differentiation (**Fig. 5B**).

All together, these results showed that activation of autophagy induced by cavin-1 deficiency contributed to insulin resistance and impaired adipogenesis.

DISCUSSION

CGL are rare diseases of diverse molecular origin which are all characterized by the association of adipose tissue deficiency with metabolic complications usually observed in obese subjects (insulin resistance, hypertriglyceridemia and liver steatosis, among others), pointing to the critical role of adipose tissue in metabolic health. Thus, defective lipid storage in adipose tissue, due to disruption of adipogenesis and/or lipid droplet formation induced by *AGPAT2* or *BSCL2* mutations,

the main molecular alterations responsible for CGL, were shown to result in insulin resistance and associated metabolic dysfunction (1). In the present study, we assessed the cellular consequences of *PTRF*/cavin-1 deficiency, responsible for rare cases of CGL. We show that the lack of cavin-1 protein expression resulted in maladaptative autophagy, which triggered insulin resistance and altered adipocyte differentiation. These results add new insights into the complex relationships between adipose tissue and whole body metabolism.

We identified two new homozygous *PTRF* mutations, predicting a point mutation or a truncation in cavin-1 (p.Asp59Val or p.Gln157Hisfs*52 alterations), in two families with CGL4, characterized by generalized lipoatrophy, insulin resistance and/or diabetes, and high levels of creatine kinase with or without symptomatic muscular dystrophy. Both mutations led to a completely abolished cavin-1 protein expression in patients'cells.

Although its physiological roles have not been completely deciphered, cavin-1 is recognized as a scaffold protein interacting with caveolin-1 both at the level of plasma caveolae and at the surface of adipocyte lipid droplet (11,14). Caveolin-1, involved in rare cases of CGL3, was shown to regulate the cellular process of autophagy (22, 27-29). Our results reveal, for the first time, that cavin-1 also contributes to the regulation of autophagy.

We first confirmed, in fibroblasts from the two probands, that cavin-1 deficiency impaired caveolae formation and expression of caveolins (8,20). More importantly, we showed that patients'cells displayed intrinsic proximal insulin signaling defects, with alterations of insulin-mediated activation of the insulin receptor and its downstream molecular targets, together with an increased autophagic flux. Recapitulation of these defects by cavin-1 knockdown, both in fibroblasts and in differentiating adipocytes, was consistent with the assumption that these alterations directly resulted from the lack of cavin-1. Interestingly, absence of caveolae, by leading to accumulation of glycosphingolipids into lysosomes, was shown to increase autophagy (12). In addition, insulin resistance and increased autophagy were previously described in caveolin-1 null mice (27,35). In accordance with these studies, we found that cavin-1 knockdown induced a decreased expression of the insulin receptor in adipocytes, which was rescued upon autophagy inhibition. Moreover, our results revealed that lack of cavin-1 also resulted in a global defect of insulin signaling pathways.

Interestingly, a decreased level of cavins induced by hypoxia was recently associated with impaired insulin signaling in adipocytes (36).

Importantly, our results show that cavin-1 deficiency impaired adipocyte differentiation and that inhibition of autophagy by *ATG5* knockdown rescued, at least partially, altered adipocyte differentiation and cellular insulin resistance. Taken together, our results strongly suggest that the metabolic defects induced by cavin-1 deficiency were mediated by a constitutive upregulation of autophagic flux. Cavin-1 could thus act as a physiological negative regulator of autophagy. ~~Consistently, autophagy which is known to regulate adipocyte differentiation and insulin sensitivity (24,25), has also been shown to contribute to lipid droplet breakdown (37). Interestingly, dysregulation of autophagy in adipose tissue could play an important role in the pathophysiology of obesity and diabetes (26).~~

Autophagy is known to regulate adipocyte differentiation, adipose brown/white remodeling and insulin sensitivity (24,25). Suppression of autophagy by systemic Atg5 or adipose-specific Atg7 knock-out in mice was previously shown to impair adipogenesis and induce lipoatrophy (24,37,38). However, increased autophagy due to the absence of cavin-1 (this study) or to caveolin-1 knock-out in mice (27) is also associated with impaired adipogenesis and lipoatrophy. In addition, autophagy was shown to be decreased (39), increased (40), or dysregulated (41) in adipose tissue from obese patients. This suggests that a finely regulated adaptative activation of autophagy is required for a proper homeostasis of adipose tissue. In accordance with our results, *IGF1R* mutations responsible for a subtype of SHORT syndrome with lipodystrophy and decreased insulin-induced Akt activation, were recently shown to activate autophagy (42). ~~This suggests that~~ Maladaptative autophagy could thus contribute to lipodystrophy and insulin resistance in several pathogenic situations.

Although further studies are needed to decipher the precise underlying mechanisms linking cavin-1 deficiency and increased autophagy, our results show that maladaptative autophagy, triggering altered adipocyte differentiation and insulin resistance, could contribute to the pathophysiology of lipoatrophy and the associated metabolic dysfunctions in CGL4. Our study add further evidence for the role of lipid droplets, their coated proteins and/or caveolae proteins in dynamic cellular functions,

including autophagy (43), and could open new therapeutic options in the field of genetic lipodystrophies and other adipose tissue diseases associated with maladaptive autophagy.

ACKNOWLEDGEMENTS

We thank the patients who participated in these studies, Drs Jean-Philippe Bastard and Soraya Fellahi from AP-HP, Department of Biochemistry, Tenon Hospital, Paris, France for leptin and adiponectin measurements, Marie-Christine Verpont, from Institut Fédératif de Recherche 65, Paris, France, for her expertise in electronic microscopy and Emilie Capel from Inserm U938, Paris, France, for technical assistance.

FIGURE LEGENDS

Figure 1. Proband-1 (A) and proband-2 (B) families and PTRF/cavin-1 molecular alterations. Patients with generalized lipodystrophy are depicted with black symbols and probands with arrows. *PTRF* sequences in control and probands are shown, with the consequences of each mutation on mRNA transcription and translation. Alignment of PTRF/cavin-1 aminoacid sequences includes the N-terminal leucine zipper domain from various species, with the conserved Asp59 residue in blue. In proband-2, *PRTF* sequencing revealed a homozygous c.471G>C transversion, affecting the last nucleotide of exon 1. Direct sequencing of cDNA derived from cultured skin fibroblasts showed that this mutation results in a splicing defect. The frameshift insertion of 143 nucleotides from intron 1, followed by a premature codon stop in exon 2, predicted the synthesis of a mutated truncated protein (p.Gln157Hisfs*52).

Figure 2. Fibroblasts from patients with CGL4 showed lack of cavin-1 protein, decreased amount of plasma membrane caveolae and increased autophagic flux

A- Protein expression of cavin-1 and its partners caveolin-1 and -2 were determined by western blot in control (Ctrl) and probands'fibroblasts (P1 and P2) as described in Methods. Beta-actin was used as an

index of the cellular protein level. A representative western blot (for each protein) is shown, with semi-quantitative analyses of western blots from experiments performed in triplicate (expressed as means ± SD). *: p< 0.05 as compared to control cells. **B-** Representative photographs of immunofluorescence microscopy. Cavin-1 was revealed by red staining (absent in probands'fibroblasts), and LC3 by green signals, either diffuse (cytosolic form of LC3-I, control cells), or punctuated (LC3-II form associated with autophagosomes, probands'cells). Cell nuclei are stained in blue with DAPI. Scale bar: 10 µm. **C, D-** Fibroblasts were examined using electron microscopy. The number of plasma membrane caveolae (C, arrows) was decreased in fibroblasts from proband-1 and absent in fibroblasts from proband-2. The number of autophagosomes (D, arrows) was increased in probands' cells (inset: magnification showing the characteristic double membrane of an autophagosome). Scale bar: 1 µm. **E, F-** Representative western blots showing the protein expression of LC3-I and LC3-II isoforms and of p62, which is degraded in lysosomes when autophagy is activated. Semi-quantitative analyses of western blots (expressed as means ± SD) show that LC3-II-to-LC3-I ratio were increased in probands'fibroblasts as compared to control cells whereas p62 was decreased, showing activation of autophagy. (E) *: p< 0.05 as compared to control cells. (F) Increased autophagic flux in patients'cells was confirmed using bafilomycin, an inhibitor of the late phase of autophagy, which increased the LC3-II-to-LC3-I ratio and increased p62 in control and patients'cells.

Figure 3. *PTRF*-mutated probands' fibroblasts showed cellular insulin resistance, and *PTRF* knockdown in control fibroblasts recapitulated increased cellular autophagy and insulin resistance

A- Insulin signaling activation was assessed in control (Ctrl) and probands'fibroblasts (P1 and P2). Representative western blots are shown, with quantification expressed as fold-stimulation by insulin of the activated/phosphorylated-to-total protein ratios (means ± SD). *: p< 0.05 as compared to control cells. IRβ: insulin receptor β-subunit, pTyr IRβ: phosphotyrosine-IRβ, pAkt: phospho-Ser473-Akt, pERK1/2: phospho-Tyr204-ERK1/2. **B-** Control fibroblasts were transfected or not with scrambled (scr) or PTRF-specific siRNA as indicated and assessed for protein expression of cavin-1, caveolin-1

and caveolin-2 as described in Methods. A representative western blot (performed in triplicate) is shown, with quantifications of the protein levels normalized to β-actin, expressed as means ± SD. *: $p < 0.05$ as compared to non-transfected cells. **C**- Western blot detection of LC3 protein isoforms LC3-I and LC3-II, p62 and β-actin (loading control), in control fibroblasts transfected or not with scrambled or PTRF-specific siRNA as indicated. Semi-quantitative analyses of LC3-II-to-LC3-I ratios and p62 levels normalized to β-actin are expressed as means ± SD. *: $p < 0.05$ as compared to non-transfected cells. **D**- Insulin signaling activation was assessed as in (**A**) in control fibroblasts transfected or not with scrambled or PTRF-specific siRNA as indicated.

Figure 4. *PTRF* mRNA silencing in 3T3-F442A preadipocytes activated autophagy, induced insulin resistance and impaired adipocyte differentiation

3T3-F442A cells were untransfected (none) or submitted to scrambled (scr) or *PTRF*-specific mRNA silencing as indicated. **A**- Representative western blots showing the effects of *PTRF* silencing on protein expression of cavin-1, caveolin-1 and caveolin-2, and on the conversion of LC3-I to LC3-II and the p62 protein amount, at D7 of adipocyte differentiation in 3T3-F442A cells. Quantifications of the protein levels normalized to β-actin are expressed as means ± SD. *: $p < 0.05$ as compared to non-transfected cells. **B**- Insulin signaling activation was assessed at D7 by evaluating insulin-induced phosphorylation of insulin receptor β-subunit, Akt and ERK1/2, normalized to the total corresponding protein content. IRβ: insulin receptor β-subunit, pTyr IRβ: phosphotyrosine-IRβ, pAkt: phospho-Ser473-Akt, pERK1/2: phospho-Tyr204-ERK1/2. **C**- Adipocyte differentiation of 3T3-F442A cells was evaluated by the protein expression of adipogenic factors (C/EBPα, PPARγ, SREBP-1c) and of the marker of mature adipocyte fatty acid synthase (FAS) at D0 and D7. A representative western blot and the quantifications of the proteins are shown, as described in (**A**) (means ± SD, *: $p < 0.05$ as compared to non-transfected cells). **D**- Oil red O-staining of intracellular stored lipids at D7 of differentiation was shown by fluorescence microscopy (cell nuclei are stained in blue with DAPI) and quantified with normalization to the total protein content as described in Methods.

Figure 5. Insulin resistance and impaired adipocyte differentiation induced by *PTRF* knockdown were partially rescued by ATG5 siRNA-mediated silencing

A- Representative western blots showing the effects of *ATG5* siRNA-mediated silencing on insulin-mediated activation of Akt and ERK1/2 in control (Ctrl) and probands' fibroblasts (P1 and P2). Cells were either untransfected or transfected with scrambled or *ATG5*-specific siRNA as indicated. Quantification was expressed as fold-stimulation by insulin of the activated/phospho-to-total protein ratios (means ± SD). *: $p < 0.05$ as compared to non-transfected cells from the same subject.

pAkt: phospho-Ser473-Akt, pERK1/2: phospho-Tyr204-ERK1/2.

B- Adipocyte differentiation of 3T3-F442A cells either untransfected, or submitted to scrambled, *PTRF* or to double *PTRF* and *ATG5* siRNA silencing, was evaluated at D7 by protein expression of adipocyte markers and Oil red O-staining of intracellular stored lipids. Representative western blots and phase-contrast microscopy images are shown. The quantifications of the proteins levels normalized to β-actin are expressed as means ± SD. Oil red O-staining was quantified with normalization to the total protein content as described in Methods. Scale bar: 1 μm. *: $p < 0.05$ as compared to non-transfected cells.

Supplemental Figure 1. Reversion of cavin-1 deficiency-mediated alterations by ATG5 knockdown in patients'fibroblasts and *PTRF*-knocked down 3T3-F442A cells

A- Autophagic flux was evaluated by LC3-II-to-LC3-I ratio and p62 levels in control and patients'cells, either untransfected, or transfected with scrambled or *ATG5*-specific siRNA as indicated. Quantifications of the protein levels normalized to β-actin are expressed as means ± SD. *: $p < 0.05$ as compared to non-transfected cells from the same subject. #: $p < 0.05$ as compared to non-transfected cells control cells.

B, C- 3T3-F442A cells either untransfected, or submitted to scrambled, *PTRF* or to double *PTRF* and *ATG5* siRNA silencing as indicated, were studied at D7 of differentiation. Autophagic flux **(B)** and activation of insulin signaling **(C)** were evaluated.

Representative western blots are shown, with quantifications expressed as protein levels normalized to

β-actin or fold-stimulation by insulin of the activated-to-total protein ratios (means ± SD).

*: p<0.05 as compared to non-transfected cells. IRβ: insulin receptor β-subunit, P-Tyr IRβ: phosphotyrosine-IRβ, pAkt: phospho-Ser473-Akt, pERK1/2: phospho-Tyr204-ERK1/2.

REFERENCES

1. Robbins AL, Savage DB. The genetics of lipid storage and human lipodystrophies. Trends Mol Med 2015; 21:433–438.

2. Kim CA, Delepine M, Boutet E, Mourabit El H, Le Lay S, Meier M, Nemani M, Bridel E, Leite CC, Bertola DR, Semple RK, O'Rahilly S, Dugail I, Capeau J, Lathrop M, Magré J. Association of a homozygous nonsense caveolin-1 mutation with Berardinelli-Seip congenital lipodystrophy. J Clin Endocrinol Metab 2008; 93:1129–1134.

3. Garg A, Kircher M, del Campo M, Amato RS, Agarwal AK. Whole exome sequencing identifies de novo heterozygous CAV1mutations associated with a novel neonatal onset lipodystrophy syndrome. Am J Med Genet 2015; 167A:1796–1806.

4. Hayashi YK, Matsuda C, Ogawa M, Goto K, Tominaga K, Mitsuhashi S, Park Y-E, Nonaka I, Hino-Fukuyo N, Haginoya K, Sugano H, Nishino I. Human PTRF mutations cause secondary deficiency of caveolins resulting in muscular dystrophy with generalized lipodystrophy. J Clin Invest 2009; 119:2623–2633.

5. Shastry S, Delgado MR, Dirik E, Turkmen M, Agarwal AK, Garg A. Congenital generalized lipodystrophy, type 4 (CGL4) associated with myopathy due to novel PTRF mutations. Am J Med Genet 2010; 152A:2245–2253.

6. Ardissone A, Bragato C, Caffi L, Blasevich F, Maestrini S, Bianchi ML, Morandi L, Moroni I, Mora M. Novel PTRF mutation in a child with mild myopathy and very mild congenital lipodystrophy. BMC Med Genet 2013; 14:1–5.

7. Murakami N, Hayashi YK, Oto Y, Shiraishi M, Itabashi H, Kudo K, Nishino I, Nonaka I, Nagai T. Congenital generalized lipodystrophy type 4 with muscular dystrophy: Clinical and pathological manifestations in early childhood. Neuromuscul Disord 2013; 23:441–444.

8. Rajab A, Straub V, McCann LJ, Seelow D, Varon R, Barresi R, Schulze A, Lucke B, Lützkendorf S, Karbasiyan M, Bachmann S, Spuler S, Schuelke M. Fatal cardiac arrhythmia and long-QT syndrome in a new form of congenital generalized lipodystrophy with muscle rippling (CGL4) Due to PTRF-CAVIN Mutations. PLoS Genet 2010; 6:1–10.

9. Dwianingsih EK, Takeshima Y, Itoh K, Yamauchi Y, Awano H, Malueka RG, Nishida A, Ota M, Yagi M, Matsuo M. A Japanese child with asymptomatic elevation of serum creatine kinase shows PTRF-CAVIN mutation matching with congenital generalized lipodystrophy type 4. Mol Genet Metab 2010; 101:233–237.

10. Jelani M, Ahmed S, Almramhi MM, Mohamoud HSA, Bakur K, Anshasi W, Wang J, Al-Aama JY. Novel nonsense mutation in the PTRF gene underlies congenital generalized lipodystrophy in a consanguineous Saudi family. Eur J Med Genet 2015; 58:216–221.

11. Kovtun O, Tillu VA, Ariotti N, Parton RG, Collins BM. Cavin family proteins and the assembly of caveolae. J Cell Sci 2015; 128:1269–1278.

12. Shvets E, Bitsikas V, Howard G, Hansen CG, Nichols BJ. Dynamic caveolae exclude bulk membrane proteins and are required for sorting of excess glycosphingolipids. Nat Commun 2015; 6:6867.

13. Hill MM, Bastiani M, Luetterforst R, Kirkham M, Kirkham A, Nixon SJ, Walser P, Abankwa D, Oorschot VM, Martin S, Hancock JF, Parton RG. PTRF-cavin, a conserved cytoplasmic protein required for caveola formation and function. Cell 2008; 132:113–124.

14. Blouin CM, Le Lay S, Eberl A, Kofeler HC, Guerrera IC, Klein C, Le Liepvre X, Lasnier F, Bourron O, Gautier JF, Ferré P, Hajduch E, Dugail I. Lipid droplet analysis in caveolin-deficient adipocytes: alterations in surface phospholipid composition and maturation defects. J Lipid Res 2010; 51:945–956.

15. Robenek H, Buers I, Robenek MJ, Hofnagel O, Ruebel A, Troyer D, Severs NJ. Topography of Lipid Droplet-Associated Proteins: insights from freeze-fracture replica Immunogold Labeling. J Lipids 2011; 2011:409371.

16. Perez-Diaz S, Johnson LA, DeKroon RM, Moreno-Navarrete JM, Alzate O, Fernandez-Real JM, Maeda N, Arbones-Mainar JM. Polymerase I and transcript release factor (PTRF) regulates adipocyte differentiation and determines adipose tissue expandability. FASEB J 2014; 28:3769–3779.

17. Cohen AW, Razani B, Schubert W, Williams TM, Wang XB, Iyengar P, Brasaemle DL, Scherer PE, Lisanti MP. Role of caveolin-1 in the modulation of lipolysis and lipid droplet formation. Diabetes 2004; 53:1261–1270.

18. Briand N, Prado C, Mabilleau G, Lasnier F, Le Liepvre X, Covington JD, Ravussin E, Le Lay S, Dugail I. Caveolin-1 expression and cavin stability regulate caveolae dynamics in adipocyte lipid store fluctuation. Diabetes 2014; 63:4032–4044.

19. Bai L, Deng X, Li J, Wang M, Li Q, An W, A D, Cong Y-S. Regulation of cellular senescence by the essential caveolar component PTRF/Cavin-1. Cell Res 2011; 21:1088–1101.

20. Liu L, Brown D, McKee M, LeBrasseur NK, Yang D, Albrecht KH, Ravid K, Pilch PF. Deletion of cavin/PTRF causes global loss of caveolae, dyslipidemia, and glucose intolerance. Cell Metab 2008; 8:310–317.

21. Ding SY, Lee MJ, Summer R, Liu L, Fried SK, Pilch PF. Pleiotropic effects of cavin-1 deficiency on lipid metabolism. J Biol Chem 2014; 289:8473–8483.

22. Castello-Cros R, Whitaker-Menezes D, Molchansky A, Purkins G, Soslowsky LJ, Beason DP, Sotgia F, Iozzo RV, Lisanti MP. Scleroderma-like properties of skin from caveolin-1-deficient mice: Implications for new treatment strategies in patients with fibrosis and systemic sclerosis. Cell Cycle 2011; 10:2140–2150.

23. Young JE1, Martinez RA, La Spada AR. Nutrient deprivation induces neuronal autophagy and implicates reduced insulin signaling in neuroprotective autophagy activation. J Biol Chem 2009; 284:2363–2373.

24. Singh R, Xiang Y, Wang Y, Baikati K, Cuervo AM, Luu YK, Tang Y, Pessin JE, Schwartz GJ, Czaja MJ. Autophagy regulates adipose mass and differentiation in mice. J Clin Invest 2009; 119:3329–3339.

25. Singh R, Kaushik S, Wang Y, Xiang Y, Novak I, Komatsu M, Tanaka K, Cuervo AM. Autophagy regulates lipid metabolism. Nature 2009; 458:1131–1137.

26. Stienstra R, Haim Y, Riahi Y, Netea M, Rudich A, Leibowitz G. Autophagy in adipose tissue and the beta cell: implications for obesity and diabetes. Diabetologia 2014; 57:1505–1516.

27. Le Lay S, Briand N, Blouin CM, Chateau D, Pradeau C, Lasnier F, Le Lièpvre X, Hajduch E, Dugail I. The lipoatrophic caveolin-1 deficient mouse model reveals autophagy in mature adipocytes. Autophagy 2010; 6:754–763.

28. Chen ZH, Cao JF, Zhou JS, Liu H, Che LQ, Mizumura K, Li W, Choi AMK, Shen HH. Interaction of caveolin-1 with ATG12-ATG5 system suppresses autophagy in lung epithelial cells. Am J Physiol Lung Cell Mol Physiol 2014; 306:L1016–L1025.

29. Shiroto T, Romero N, Sugiyama T, Sartoretto JL, Kalwa H, Yan Z, Shimokawa H, Michel T. Caveolin-1 Is a critical determinant of autophagy, metabolic switching, and oxidative stress in vascular endothelium. PLoS One 2014; 9: e87871.

30. Bidault G, Garcia M, Vantyghem M-C, Ducluzeau P-H, Morichon R, Thiyagarajah K, Moritz S, Capeau J, Vigouroux C, Bereziat V. Lipodystrophy-linked LMNA p.R482W mutation induces clinical early atherosclerosis and in vitro endothelial dysfunction. Arterioscler Thromb Vasc Biol 2013; 33:2162–2171.

31. Caron M, Auclair M, Vigouroux C, Glorian M, Forest C, Capeau J. The HIV protease inhibitor indinavir impairs sterol regulatory element-binding protein-1 intranuclear localization, inhibits preadipocyte differentiation, and induces insulin resistance. Diabetes 2001; 50:1378–1388.

32. Kimura S, Noda T, Yoshimori T. Dynein-dependent movement of autophagosomes mediates efficient encounters with lysosomes. Cell Struct Funct 2008; 33:109-122.

33. Barth S, Glick D, Macleod KF. Autophagy: assays and artifacts. J Pathol 2010; 221:117–124.

34. Glick D, Barth S, Macleod KF. Autophagy: cellular and molecular mechanisms. J Pathol 2010; 221:3–12.

35. Cohen AW, Razani B, Wang XB, Combs TP, Williams TM, Scherer PE, Lisanti MP. Caveolin-1-deficient mice show insulin resistance and defective insulin receptor protein expression in adipose tissue. Am J Physiol Cell Physiol 2003; 285:C222-C235.

36. Regazzetti C, Dumas K, Lacas-Gervais S, Pastor F, Peraldi P, Bonnafous S, Dugail I, Le Lay S, Valet P, Le Marchand-Brustel Y, Tran A, Gual P, Tanti J-F, Cormont M, Giorgetti-Peraldi S. Hypoxia inhibits cavin-1 and cavin-2 expression and down-regulates caveolae in adipocytes. Endocrinology 2015; 156:789–801.

~~37. Martinez-Lopez N, Singh R. Autophagy and lipid droplets in the liver. Annu Rev Nutr 2015; 35:215–237.~~

37. Zhang Y, Goldman S, Baerga R, Zhao Y, Komatsu M, Jin S. Adipose-specific deletion of autophagy-related gene 7 (atg7) in mice reveals a role in adipogenesis. Proc Natl Acad Sci U S A 2009; 106:19860-19865.

38. Baerga R, Zhang Y, Chen PH, Goldman S, Jin S. Targeted deletion of autophagy-related 5 (atg5) impairs adipogenesis in a cellular model and in mice. Autophagy 2009; 5:1118-1130.

39. Soussi H, Reggio S, Alili R, Prado C, Mutel S, Pini M, Rouault C, Clément K, Dugail I. DAPK2 Downregulation Associates With Attenuated Adipocyte Autophagic Clearance in

Human Obesity. Diabetes 2015; 64:3452-3463.

40. Jansen HJ, van Essen P, Koenen T, Joosten LA, Netea MG, Tack CJ, Stienstra R. Autophagy activity is up-regulated in adipose tissue of obese individuals and modulates proinflammatory cytokine expression. Endocrinology 2012; 153:5866-5874.

41. Nuñez CE, Rodrigues VS, Gomes FS, Moura RF, Victorio SC, Bombassaro B, Chaim EA, Pareja JC, Geloneze B, Velloso LA, Araujo EP. Defective regulation of adipose tissue autophagy in obesity. Int J Obes (Lond) 2013; 37:1473-1480.

42. Prontera P, Micale L, Verrotti A, Napolioni V, Stangoni G, Merla G. A new homozygous IGF1R variant defines a clinically recognizable incomplete dominant form of SHORT Syndrome. Hum Mutat 2015; 36:1043-1047.

43. Barbosa AD, Savage DB, Siniossoglou S. Lipid droplet–organelle interactions: emerging roles in lipid metabolism. Curr Opin Cell Biol 2015; 35:91–97.

Table 1

Characteristics of patients with *PTRF* homozygous mutations.

	Proband-1	**Proband-2**	**Sister 1 of Proband-2**	**Sister 2 of Proband-2**	**Reference ranges**
***PTRF* homozygous mutation**	p.D59V	p.Q157HfsX52	p.Q157HfsX52	p.Q157HfsX52	
Age at examination (years)	32	13	6	2	
Sex	Female	Female	Female	Female	
BMI (kg/m^2) (Z-score in children)	19.2	17.5 (-0.47)	15.4 (0.13)	16.1 (-0.24)	
Lipodystrophy	Congenital Generalized	Congenital Generalized	Congenital Generalized	Congenital Generalized	
Acanthosis nigricans	Neck, axillae	Neck, axillae	-	No	
Mental retardation	Mild	Mild	No	No	
Muscular signs	Generalized muscular hypertrophy, cramps	Generalized muscular hypertrophy	Calf hypertrophy, generalized muscle weakness	Generalized muscle weakness	
Cardiac examination	Normal	Normal	Normal	Normal	
Creatine kinase (IU/L)	308	1054	618	1202	15-95
Fasting glucose (mmol/L)	9.5	4.5	4.2	4.3	4-5.6
Fasting insulin (mIU/L)	Insulin-treated	16.3	9.2	4.5	2-10
Triglyceride (mmol/L)	2.3	1.7	0.7	1.0	0.4-1.5
Total cholesterol (mmol/L)	4.3	3.4	3.5	3.7	4.1-6.2
HDL-cholesterol (mmol/L)	0.4	0.7	0.9	0.8	1.3-2.1
Leptin (µg/L)	3.2	0.2	0.2	0.7	4-20
Adiponectin (mg/L)	2.8	0.9	1.7	2.8	3.9-12.9
Liver enzymes (AST/ALT) (IU/L)	32/34	43/53	44/60	43/52	5-35 / 5-35
Liver examination	Hepatomegaly and steatosis (histology)	Hepatomegaly	Hepatomegaly	-	

BMI, body mass index; AST: aspartate aminotransferase; ALT: alanine aminotransferase

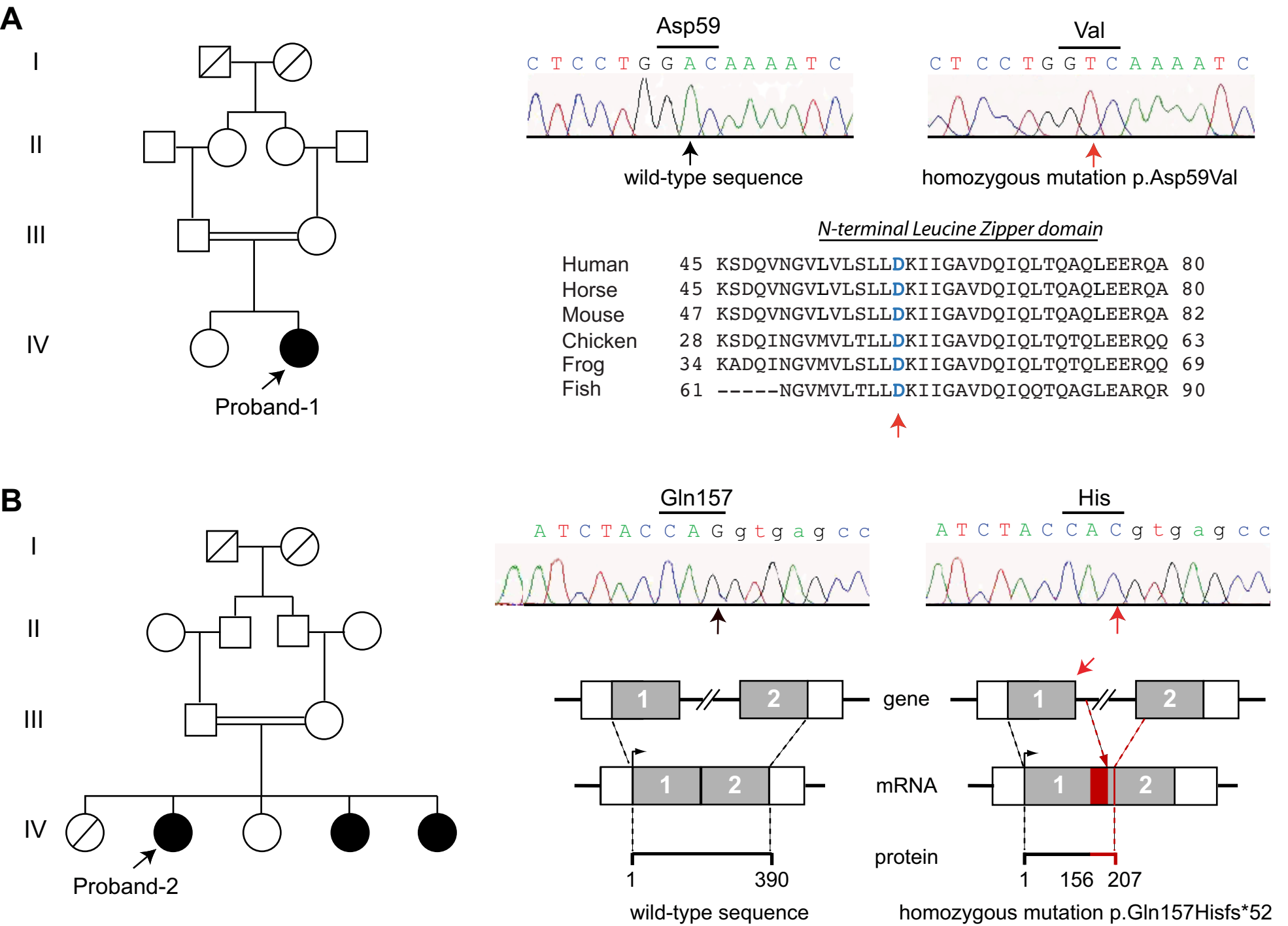
A
I
II
III
IV
Proband-1
Asp59
C T C C T G G A C A A A A T C
wild-type sequence
Val
C T C C T G G T C A A A A T C
homozygous mutation p.Asp59Val
N-terminal Leucine Zipper domain
Human 45 KSDQVNGVLVLSLLDKIIGAVDQIQLTQAQLEERQA 80
Horse 45 KSDQVNGVLVLSLLDKIIGAVDQIQLTQAQLEERQA 80
Mouse 47 KSDQVNGVLVLSLLDKIIGAVDQIQLTQAQLEERQA 82
Chicken 28 KSDQINGVMVLTLLDKIIGAVDQIQLTQTQLEERQQ 63
Frog 34 KADQINGVMVLSLLDKIIGAVDQIQLTQTQLEERQQ 69
Fish 61 -----NGVMVLTLLDKIIGAVDQIQQTQAGLEARQR 90
B
I
II
III
IV
Proband-2
Gln157
A T C T A C C A G g t g a g c c
His
A T C T A C C A C g t g a g c c
gene
mRNA
protein
1
2
1
390
1
156
207
wild-type sequence
homozygous mutation p.Gln157Hisfs*52

Figure 1

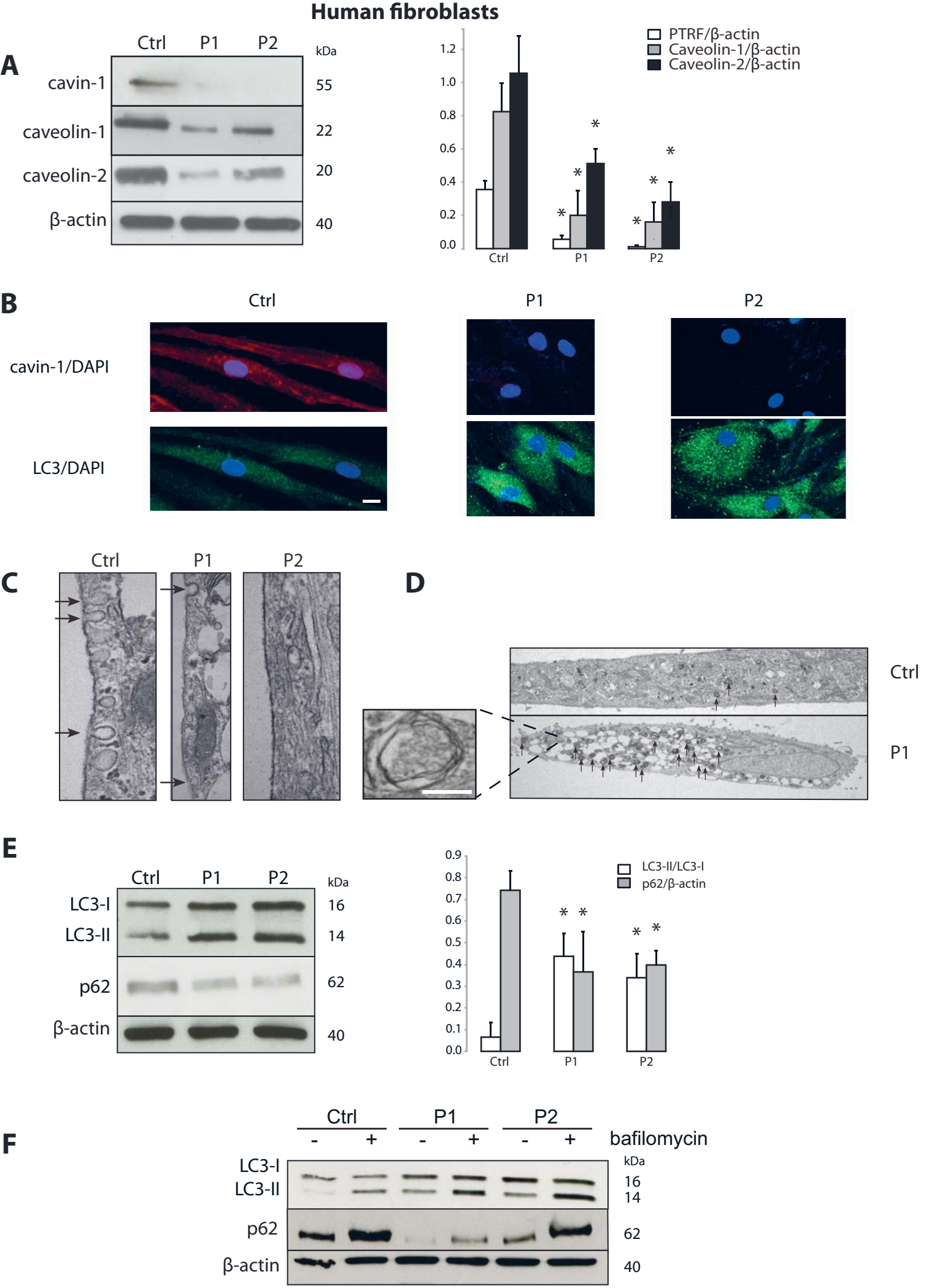
Human fibroblasts
A
Ctrl
P1
P2
kDa
cavin-1
caveolin-1
caveolin-2
β-actin
55
22
20
40
PTRF/β-actin
Caveolin-1/β-actin
Caveolin-2/β-actin
1.2
1.0
0.8
0.6
0.4
0.2
0.0
Ctrl
P1
P2
B
Ctrl
P1
P2
cavin-1/DAPI
LC3/DAPI
C
Ctrl
P1
P2
D
Ctrl
P1
E
Ctrl
P1
P2
kDa
LC3-I
LC3-II
p62
β-actin
16
14
62
40
LC3-II/LC3-I
p62/β-actin
0.9
0.8
0.7
0.6
0.5
0.4
0.3
0.2
0.1
0.0
Ctrl
P1
P2
F
Ctrl
P1
P2
-
+
-
+
-
+
bafilomycin
kDa
LC3-I
LC3-II
p62
β-actin
16
14
62
40

Figure 2

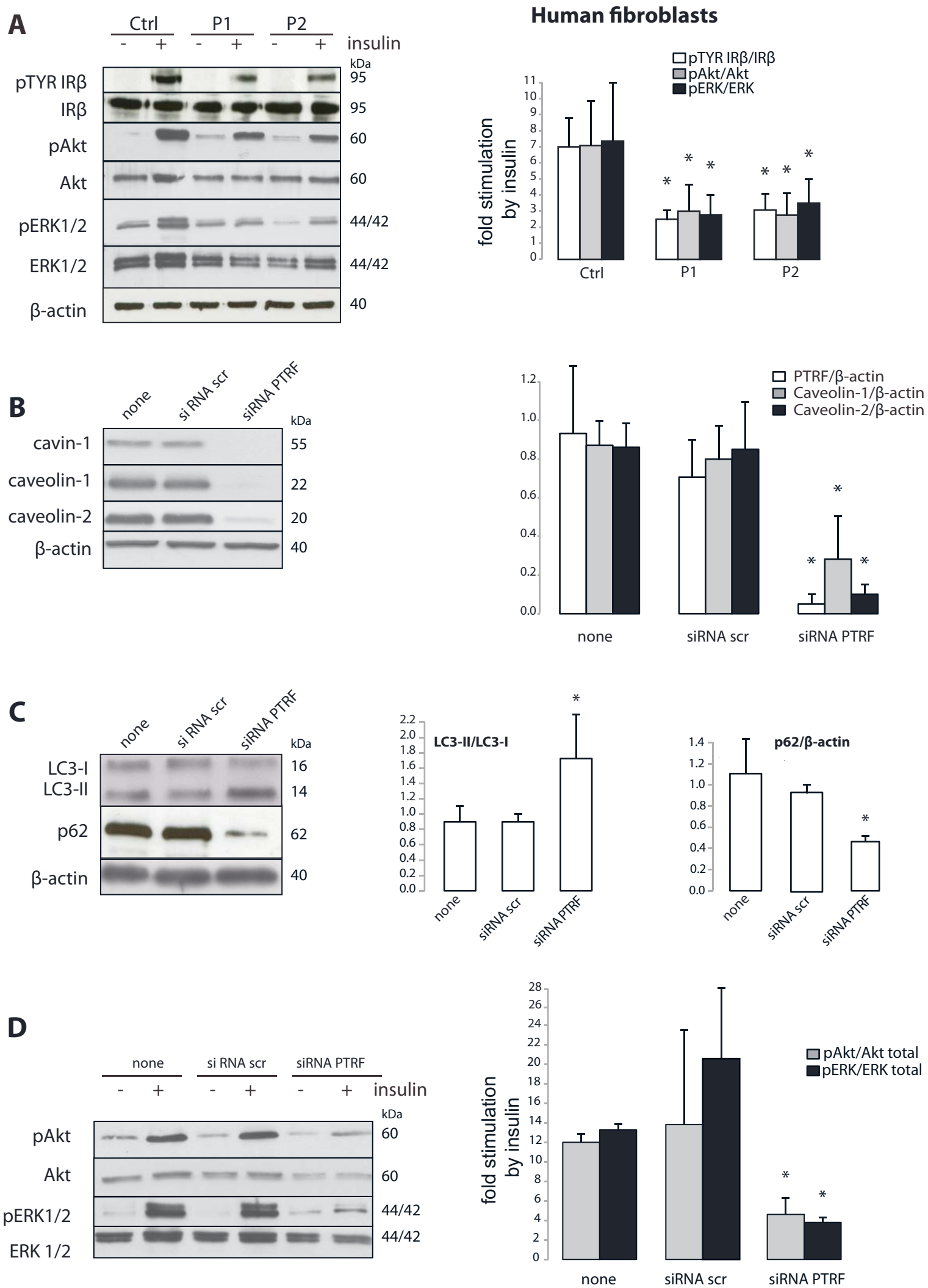
A
Human fibroblasts
Ctrl
P1
P2
insulin
kDa
pTYR IRβ
IRβ
pAkt
Akt
pERK1/2
ERK1/2
β-actin
95
95
60
60
44/42
44/42
40
pTYR IRβ/IRβ
pAkt/Akt
pERK/ERK
fold stimulation by insulin
B
none
si RNA scr
siRNA PTRF
cavin-1
caveolin-1
caveolin-2
55
22
20
PTRF/β-actin
Caveolin-1/β-actin
Caveolin-2/β-actin
C
LC3-I
LC3-II
p62
16
14
62
LC3-II/LC3-I
p62/β-actin
D
pAkt/Akt total
pERK/ERK total

Figure 3

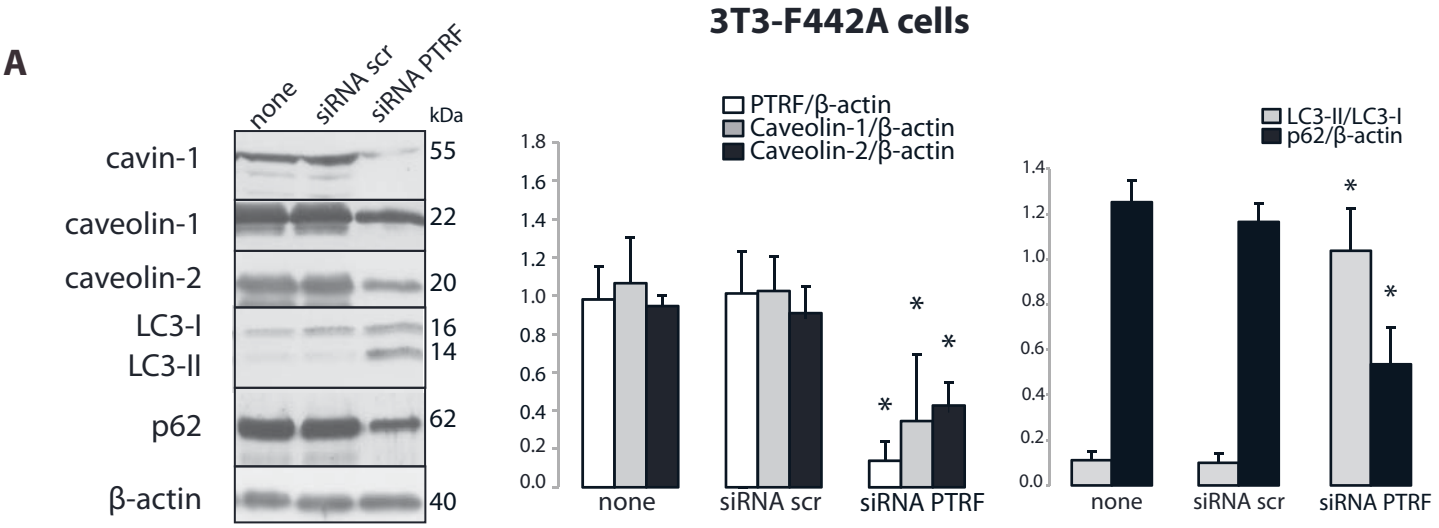
3T3-F442A cells
A
none
siRNA scr
siRNA PTRF
kDa
cavin-1
caveolin-1
caveolin-2
LC3-I
LC3-II
p62
β-actin
55
22
20
16
14
62
40
PTRF/β-actin
Caveolin-1/β-actin
Caveolin-2/β-actin
LC3-II/LC3-I
p62/β-actin
none
siRNA scr
siRNA PTRF

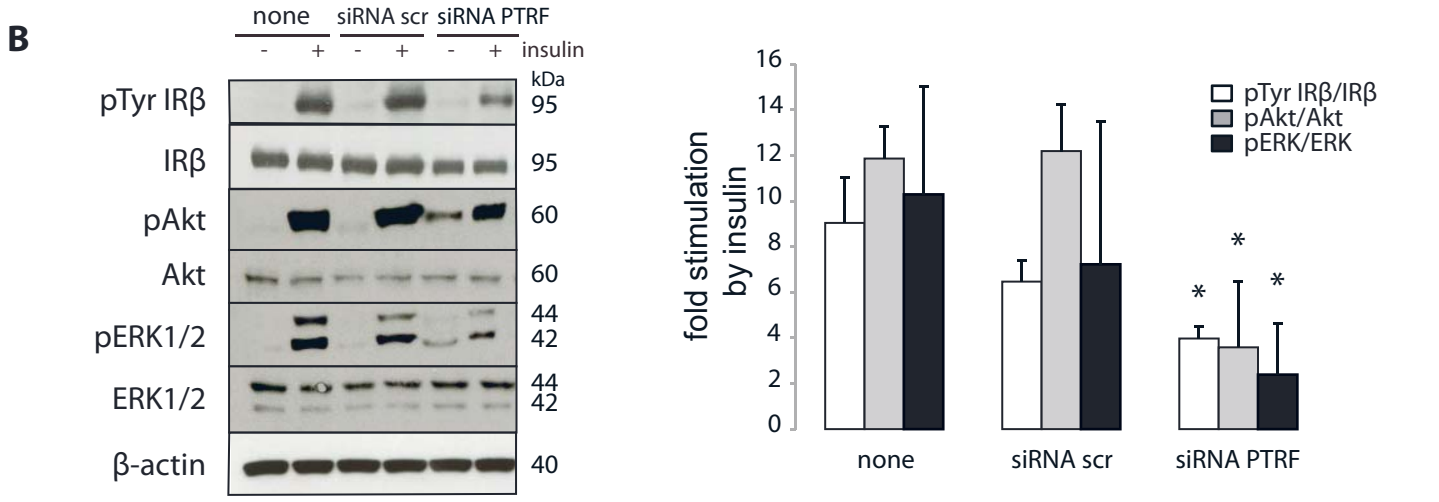
B
none
siRNA scr
siRNA PTRF
insulin
kDa
pTyr IRβ
IRβ
pAkt
Akt
pERK1/2
ERK1/2
β-actin
95
95
60
60
44
42
44
42
40
fold stimulation by insulin
pTyr IRβ/IRβ
pAkt/Akt
pERK/ERK
none
siRNA scr
siRNA PTRF

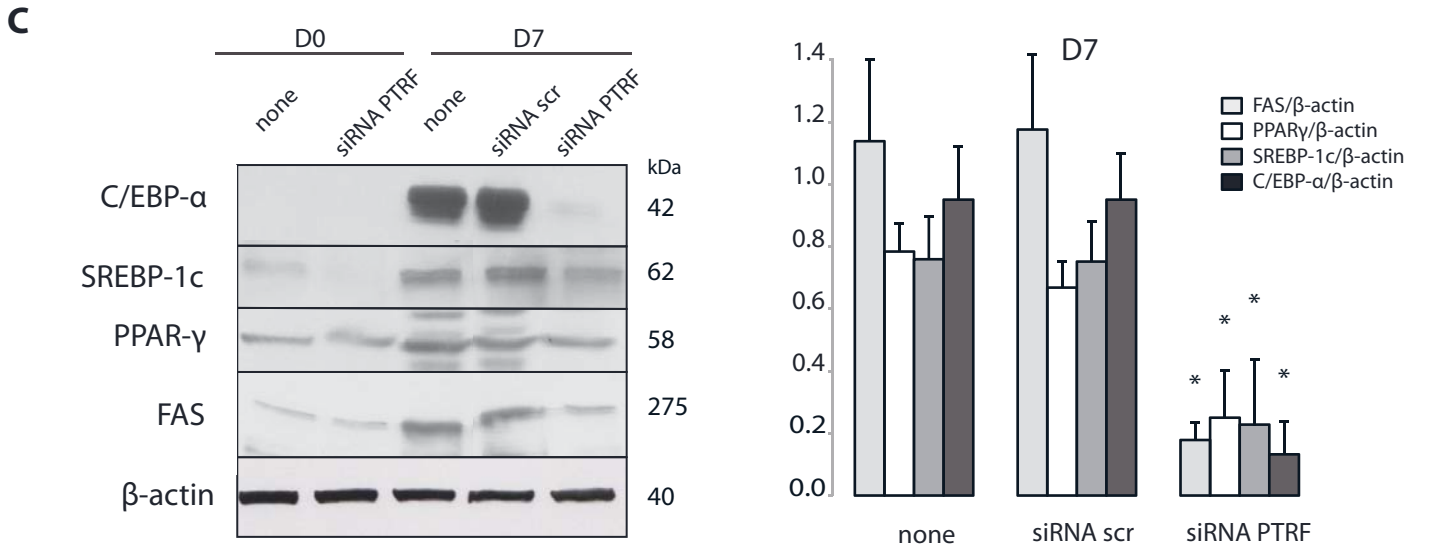
C
D0
D7
none
siRNA PTRF
none
siRNA scr
siRNA PTRF
kDa
C/EBP-α
SREBP-1c
PPAR-γ
FAS
β-actin
42
62
58
275
40
D7
FAS/β-actin
PPARγ/β-actin
SREBP-1c/β-actin
C/EBP-α/β-actin
none
siRNA scr
siRNA PTRF


D
none
siRNA scr
siRNA PTRF
Red oil/total protein level
none
si RNA scr
siRNA PTRF

Figure 4

A Human fibroblasts

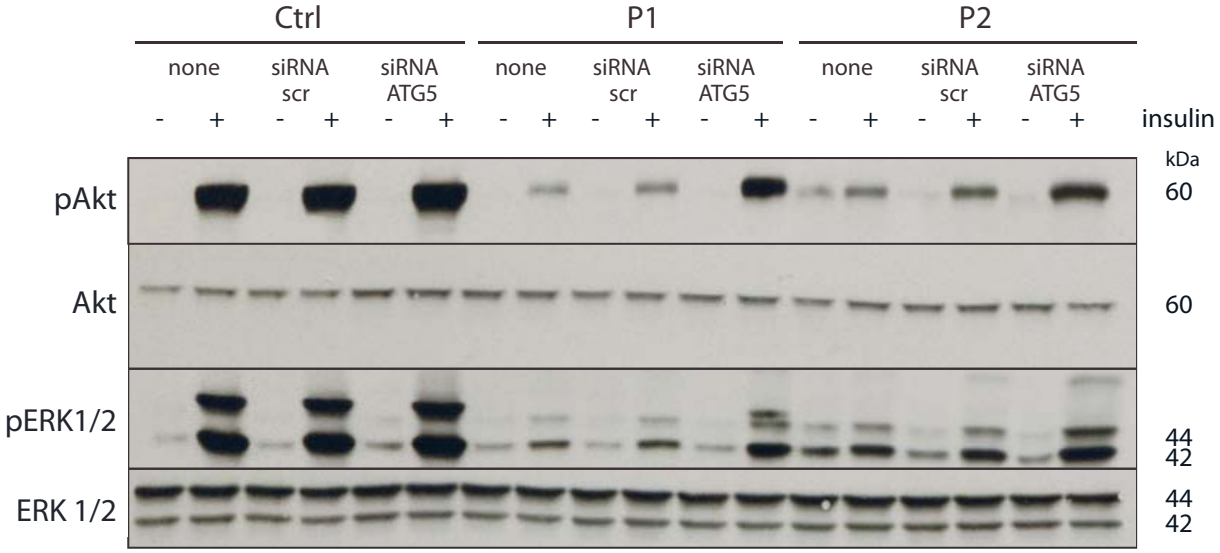

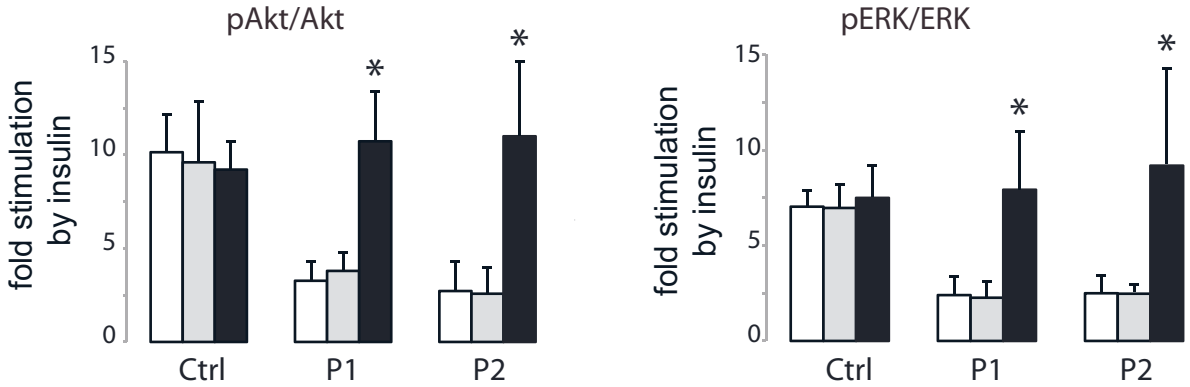

B 3T3-F442A cells at D7 of adipocyte differentiation

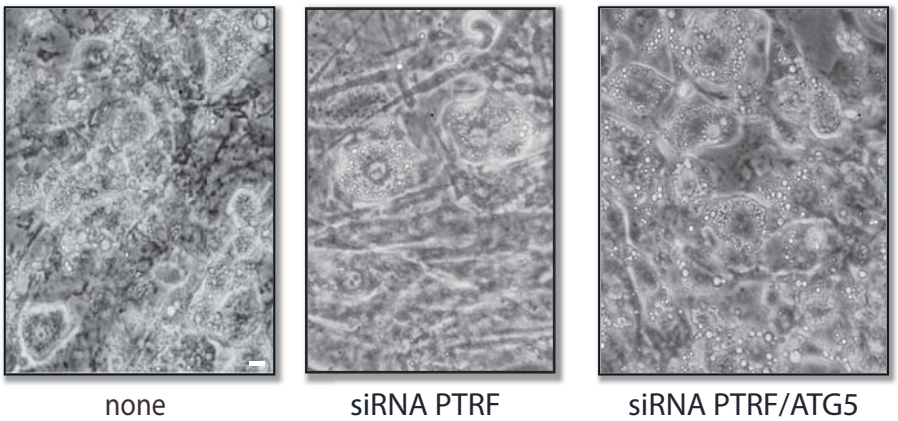

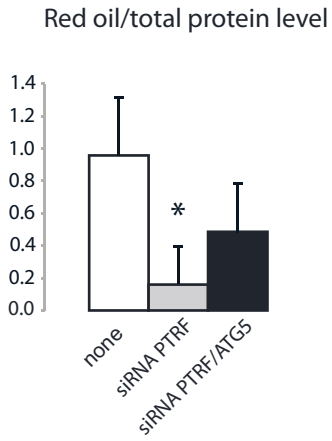

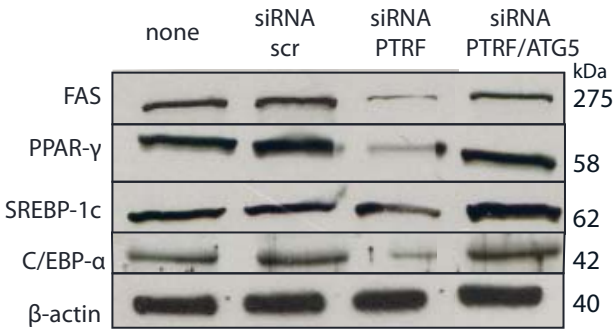

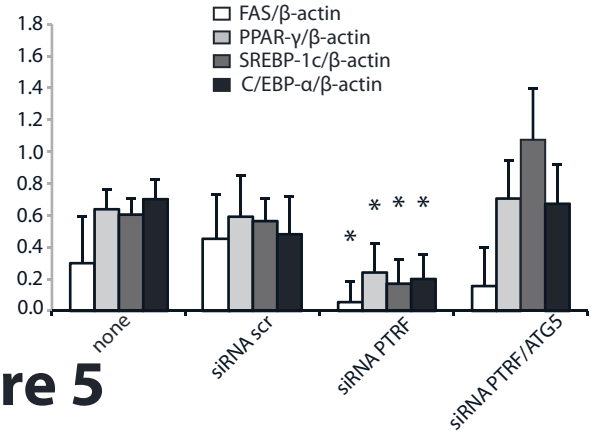

Figure 5